



# Vibration suppression of thin-walled workpiece milling using a time-space varying PD control method via piezoelectric actuator

Shuyu Wang<sup>1</sup> · Qinghua Song<sup>1,2</sup> · Zhanqiang Liu<sup>1,2</sup>

Received: 7 April 2019 / Accepted: 20 September 2019 / Published online: 8 November 2019  
© Springer-Verlag London Ltd., part of Springer Nature 2019

## Abstract

The vibration suppression and workpiece surface improvement of thin-walled workpiece milling are highly concerned due to the weak stiffness of the workpiece and the time variant of dynamic characteristics during milling process. In this paper, an active vibration control system is developed to suppress the vibration of thin-walled workpiece milling. The dynamic model of plate-actuator milling system is derived using Hamilton's principle and solved using FEM method. Acceleration sensor and piezoelectric patch are selected as the sensor and actuator in the control system. Considering the time variant of dynamic characteristics and the position limit of sensor and actuator during milling process, a time-space varying PD (VPD) control method is presented and utilized. The VPD control method applies time varying control parameters. Some simulation and experimental validations are carried out to validate the effectiveness of the control system. The overall results indicate that the proposed control system perform well in suppressing the vibration of thin-walled workpiece milling process.

**Keywords** Vibration control · Thin-walled workpiece milling · Piezoelectric actuator · PD control

## 1 Introduction

Thin-walled components with complex shape and light weight characteristics play an important role in many applications such as military and aerospace industries. In the processing of the thin-walled workpiece, the machining vibration of thin-walled workpiece is an undesirable phenomenon, which could cause negative influences such as disturbing the accuracy of the final workpiece, the production efficiency, and the life of machine spindles as well as cutters. Therefore, to achieve the

high performance of products, analysis and suppression of the machining vibration are of great importance in the thin-walled workpiece machining process. Thin-walled workpiece milling has received special attention due to its great significance in machining flexible workpiece such as aeroengine blades, casings, and blisks. However, low rigidity, high flexibility, and large machining deformation of the workpiece, as well as the time-varying dynamic characteristics of the milling process could induce severe vibration. Therefore, it is necessary to investigate and suppress the machining vibration in thin-walled milling process.

For the effort of suppressing the vibration in cutting process, numerous researches were made in the past decades. For instance, Altintas and Budak [1, 2] presented an analytical method based on zero order Fourier transform of cutting force to predict the milling stability lobes. Zhou et al. [3] proposed an analytical model considering tool-workpiece engagement region and different cutter lead angles for chatter stability prediction. According to the stable region in the SLD (stability lobes diagram), the optimal cutting parameter (spindle speed and axial depth) needs to be identified and selected to avoid chatter. However, to predict the stable cutting parameter regions, certain characteristics of the cutting process are necessary. It means some stability strategies based on stable cutting parameter region, such as the spindle speed variation strategy,

✉ Qinghua Song  
ssinghua@sdu.edu.cn

Shuyu Wang  
wsy1023@yeah.net

Zhanqiang Liu  
melius@sdu.edu.cn

<sup>1</sup> Key Laboratory of High Efficiency and Clean Mechanical Manufacture, Ministry of Education, School of Mechanical Engineering, Shandong University, Jinan, People's Republic of China

<sup>2</sup> National Demonstration Center for Experimental Mechanical Engineering Education, Shandong University, Jinan, People's Republic of China

are cumbersome for general applications [4]. Besides, there are also many researches devoted to use passive vibration control methods to reduce the machining vibration. Liu et al. [5] presented a dynamic absorber applied to a 2-DOF milling tool and verified the model by numerical simulation. Sathianarayanan et al. [6] and Mei et al. [7, 8] also discussed on approaches of adjusting the stiffness of boring bar by using magnetorheological fluids, which perform well in reducing machining vibration. Wan et al. [9] proposed a prestressing method to improve the chatter stability of thin-walled milling process. Shamoto et al. [10] presented a novel milling trajectory planning to suppress chatter vibration, which is machining flexible plates by simultaneous double-sided milling. They prove that the application of additional mass or damping layer attached on the surface of workpiece or tool is also a good passive control way to suppress vibration or improve stability during machining process. Kolluru et al. [11] proposed a new surface damping method (which attached distributed discrete masses large thin-walled casings as viscoelastic layer) for reducing the machining vibrations. Wan et al. [12] presented an additional masses attaching method to optimize and improve the stable processing condition of thin-walled milling process. Yuan et al. [13] designed a novel tunable mass damper for alleviating vibrations in milling of cylindrical parts. Wang et al. [14] present a stiffness variation method using piezoelectric stack actuators applied on milling cutter to suppress milling chatter. Apart from the passive vibration control methods, the active vibration control method on cutting process has received increasing attentions from researchers.

Current researches on active vibration control method in cutting process mainly include two types. One is applying active damping to the cutting system [15], and the other is directly eliminating the cutting vibrations using various actuators. For the former method, the designed active damping is applied to the cutting process at the natural frequencies of the control objects, so that the damped modes could be greatly stabilized [16–18]. For the control method of directly eliminating the cutting vibration, researchers make the actuators drive the tool or workpiece moving along the opposite direction of the cutting vibrations. For example, El-Sinawi and Kashani [19] developed an optimal vibration control system for turning operations by using active tool holder. Experimental results confirmed the performance in vibration elimination and machining quality improvement. Brecher et al. [20] proposed an active workpiece holder with two high dynamic axes controlled by piezoelectric actuators onto a milling machine. This allows for compensation of spindle vibrations that caused instabilities during the cutting process. da Silva et al. [21] have numerically exploited a velocity feedback control scheme which use piezoelectric patches embedded on tool holders to suppress cutting vibration. Similarly, Tanaka et al. [22] experimentally investigated the control

method for suppressing vibrations using piezoelectric actuators. Using piezoelectric elements as sensor or actuator to improve structural behavior, especially suppress vibration of structure, has been seen in many researches. The pioneering work on the application of piezoelectric patch was done by Crawley and de Luis [23]; they developed the first analytical model for embedded or surface bonded piezoelectric elements. Besides the selection of actuator and sensor, the control method design is also important in the whole vibration control system. Closed-loop control is considered as an effective choice, and the control algorithm of the closed-loop controllers is a key problem and research focus of the control system. For example, Rofooei et al. [24] presented a method using linear classical optimal control algorithm with displacement-velocity feedback to control the dynamic response of a thin rectangular plate by active piezoelectric actuators. Qiu et al. [25] investigated the application of piezoelectric actuators with acceleration sensor-based proportional control for vibration suppression of a flexible beam.

For thin-walled workpiece milling, the relative space location between cutter and workpiece is time varying, which makes the dynamic characteristics of cutting process time varying with the motion of the cutter [26, 27]. In the above research efforts, control effects are acted on either the tool holder or a selected point of workpiece, and hence, a suitable control method for the condition of cutting location varying during the milling process is not available in the literature.

Therefore, the main purpose of this paper is to propose an effective method to control the cutting vibration in thin-walled milling process with the application of piezoelectric materials as actuators, and the control algorithm should consider the engagement position between cutter and workpiece and the time-varying dynamic characteristics of thin-walled milling system. The organization of this article is as follows. In Sect. 2, the model of thin-walled plate milling with vibration control by piezoelectric actuator is derived. In Sect. 3, a control system including design of connection of apparatus and the acceleration feedback-based time-varying PD control algorithm is presented. In Sect. 4, some simulations of numerical examples and milling experiments are conducted to validate the efficiency of the proposed vibration control system. Finally, the conclusions are drawn in the last section.

## 2 Model of thin-walled plate milling with vibration control by piezoelectric actuator

### 2.1 Motion equation of plate-actuator milling system

To control the vibration of thin plate milling process, piezoelectric patch is attached on the thin-plate workpieces, and an analytical model of thin plate milling process with the

application of vibration control by piezoelectric actuator is built. As shown in Fig. 1, during the milling process, the cutter is moving along its milling trajectory. The thin plate is one edge clamped with length of  $L$ , width of  $W$ , and thickness of  $h_p$ .  $u_1, u_2$  and  $v_1, v_2$  denote the location of piezoelectric patch on the surface of thin plate along  $x$ -axis and  $y$ -axis, respectively. The thickness of piezoelectric patch is  $h_a$ . Due to the high flexibility of thin plate in one direction (transverse direction), one degree of freedom model was usually assumed, and  $w(x, y, t)$  denotes the deflection of the mid-plane of the plate at any point and at any time  $t$ .

In this part, a motion equation of the dynamic model is obtained. The motion equation of thin plate with piezoelectric patch is derived based on Kirchhoff theory by assuming the following conditions:

1. The thickness of the plate ( $h_p$ ) is small compared to its lateral dimensions.
2. The middle plane of the plate does not undergo in-plane deformation. Thus, the midplane remains as the neutral plane after deformation or bending.
3. The displacement components of the mid-surface of the plate are small compared to the thickness of the plate.
4. The influence of transverse shear deformation is neglected.
5. The transverse normal strain under transverse loading can be neglected.

Moreover, as the thickness and area of the piezoelectric patch is very small in comparison to those of the thin plate workpiece, it can be assumed that the bending stiffness and inertial effect of the piezoelectric patch are negligible.

When the voltage is applied, the piezoelectric actuators could produce an induce tension along  $x$ -axis and  $y$ -axis, so the only parameter of piezoelectric actuator which be considered has effect on the plate-actuator system is the strain energy

of the piezoelectric patch due to the tension. When applied with voltage, the strain energy of the piezoelectric patch due to the tension can be expressed as follows:

$$U_a = \frac{1}{2} \int_{u_1}^{u_2} \int_{v_1}^{v_2} \left\{ [h_{31}h_a\bar{D}_3(h_a + h_p)] \left( \frac{\partial^2 w}{\partial x^2} + \frac{\partial^2 w}{\partial y^2} \right) + h_a\beta_{33}^T \bar{D}_3 \right\} dx dy \tag{1}$$

In the above equation,  $h_{31}, \bar{D}_3$ , and  $\beta_{33}^T$  are the piezoelectric constant, electrical displacement, and the dielectric constant measured under a constant electrical field, respectively.

In this analysis, the strain energy is considered to be uniformly distributed over the whole piezoelectric patch and the step function is used to express the strain energy of the actuator over the area of thin plate:

$$U_a = \frac{1}{2} \iint_A \left\{ [h_{31}h_a\bar{D}_3(h_a + h_p)] \left( \frac{\partial^2 w}{\partial x^2} + \frac{\partial^2 w}{\partial y^2} \right) + h_a\beta_{33}^T \bar{D}_3 \right\} \Delta H_u(x)\Delta H_v(y) dx dy \tag{2}$$

In the above equation:

$$\Delta H_u(x) = H(x-u_1) - H(x-u_2) \tag{3}$$

$$\Delta H_v(y) = H(y-v_1) - H(y-v_2) \tag{4}$$

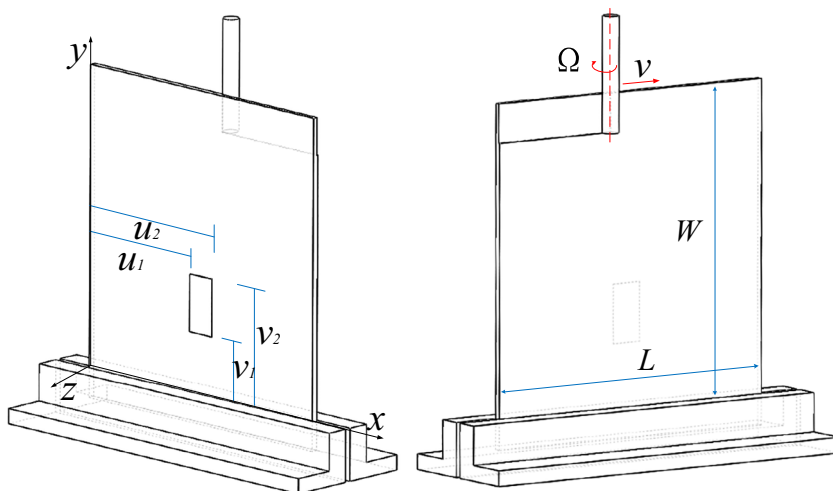
The inertial effect of the piezoelectric patch is neglected, so the kinetic energy of the plate-actuator system is assumed to only contain that of the thin plate ( $T$ ). The kinetic energy of the plate is written as follows:

$$T = \frac{\rho h_p}{2} \iint_A \left( \frac{\partial w}{\partial t} \right)^2 dx dy \tag{5}$$

where  $\rho$  denotes the density of the thin plate.

The strain energy of the system is assumed to contain that of the thin plate ( $\pi$ ) and that of the piezoelectric patch due to tension ( $U_a$ ).

Fig. 1 Model of the piezo patch-thin plate system



The strain energy of plate could be written as follows

$$\pi = \frac{D}{2} \iint_A \left\{ \left( \frac{\partial^2 w}{\partial x^2} + \frac{\partial^2 w}{\partial y^2} \right)^2 - 2(1-\nu) \left[ \frac{\partial^2 w}{\partial x^2} \frac{\partial^2 w}{\partial y^2} - \left( \frac{\partial^2 w}{\partial x \partial y} \right)^2 \right] \right\} dx dy \quad (6)$$

in which  $D$  represents the flexural rigidity of the plate:

$$D = \frac{Eh_p^3}{12(1-\nu^2)} \quad (7)$$

where  $E$  and  $\nu$  is Young’s modulus and Poisson’s ratio of the thin plate, respectively.

There is an external force, which represents the milling force,  $f(x,y,t)$ , acting on the plate, as shown in Fig. 2, and the milling force in the  $z$ -direction is expressed as follows:

$$f = \frac{1}{2} a_p a_e K_t \sum_{j=0}^{N-1} g_j [\sin 2\phi_j - K_r (1 + \cos 2\phi_j)] \quad (8)$$

where  $a_p$  is axial depth of cut,  $a_e$  is the radial depth of cut,  $K_t$  is cutting force coefficient,  $K_r$  is ratio of cutting force coefficient,  $g_j$  is the screen function, and  $\phi_j$  is the instantaneous immersion angle of the  $j$ th tooth.

The work done by the milling force ( $W_f$ ) is given by the following:

$$W_f = \iint_A f w dx dy \quad (9)$$

The equation of motion can be derived by applying the generalized Hamilton’s principle:

$$\delta \int_{t_1}^{t_2} L dt = \delta \int_{t_1}^{t_2} (\pi + U_a - W_f - T) dt = 0 \quad (10)$$

Substituting Eqs. (2), (5), (6), and (9) into Eq. (10), the motion equation of the thin plate with piezoelectric actuator and the associated boundary conditions are obtained as follows:

$$D \left( \frac{\partial^4 w}{\partial x^4} + 2 \frac{\partial^4 w}{\partial x^2 \partial y^2} + \frac{\partial^4 w}{\partial y^4} \right) + \rho h_p \ddot{w} = f(x,y,t) - \frac{1}{2} h_{31} h_a \bar{D}_{31} (h_a + h_p) [\Delta \delta'_u(x) \Delta H_v(y) + \Delta H_u(x) \Delta \delta'_v(y)] \quad (11)$$

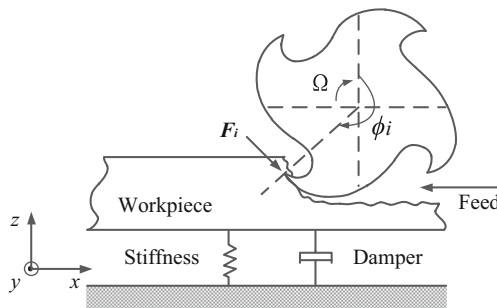


Fig. 2 Cutting process

where  $\Delta \delta'_u$  and  $\Delta \delta'_v$  is the first derivative of  $\Delta \delta_u$  and  $\Delta \delta_v$  respectively, and

$$\Delta \delta_u = \delta(x-u_1) - \delta(x-u_2) \quad (12)$$

$$\Delta \delta_v = \delta(y-v_1) - \delta(y-v_2) \quad (13)$$

$\delta(x)$  is the Dirac-delta function.

Moreover, based on the research [23] about the relationship between the characteristic and applied voltage of the piezoelectric patch, the following equation is obtained:

$$\bar{D}_3 = \frac{E_p^E d_{31} V(t)}{(1-\nu_p) h_a} \quad (14)$$

where  $E_p^E$  and  $\nu_p$  are the elastic modulus and Poisson’s ratio of the piezoelectric patch, and  $V$  denotes the voltage applied on the piezoelectric patch at time  $t$ .

Substituting the Eq. (14) into Eq. (11), the motion equation of the plate-actuator system containing the applied voltage could be written as follows:

$$D \left( \frac{\partial^4 w}{\partial x^4} + 2 \frac{\partial^4 w}{\partial x^2 \partial y^2} + \frac{\partial^4 w}{\partial y^4} \right) + \rho h_p \ddot{w} = f(x,y,t) - q V(t) [\Delta \delta'_u(x) \Delta H_v(y) + \Delta H_u(x) \Delta \delta'_v(y)] \quad (15)$$

where  $q$  denotes some characteristic constants of the plate-actuator system with the following:

$$q = \frac{h_{31} (h_a + h_p) E_p^E d_{31}}{2(1-\nu_p)} \quad (16)$$

### 2.2 Solution to the equation of motion

In this part, the finite element method (FEM) is utilized to solve the motion equation of the thin plate with piezoelectric actuator. For this, a four-node Kirchhoff plate element is assumed and three degrees of freedom (lateral deflection rotation along the  $x$ -axis and rotation along the  $y$ -axis) are assigned to each node. According to the weighted residual method, the final weak form of Eq. (15) over an element ( $x_b - x_a, y_b - a$ ) is constructed as follows:

$$0 = \int_{x_a}^{x_b} \int_{y_a}^{y_b} \left[ D \frac{\partial^2 v}{\partial x^2} \frac{\partial^2 w}{\partial x^2} + 2D \frac{\partial^2 v}{\partial x \partial y} \frac{\partial^2 w}{\partial x \partial y} + D \frac{\partial^2 v}{\partial y^2} \frac{\partial^2 w}{\partial y^2} + \nu \rho h_p \frac{\partial^2 w}{\partial t^2} - v f + v q V (\Delta \delta'_u \Delta H_v + \Delta H_u \Delta \delta'_v) \right] dx dy + D \left( \int_{r_c}^{-\nu} \frac{\partial^3 w}{\partial y^3} + \frac{\partial v}{\partial y} \frac{\partial^2 w}{\partial y^2} + 2 \frac{\partial v}{\partial x} \frac{\partial^2 w}{\partial x \partial y} dx + \int_{r_c}^{\nu} \frac{\partial^3 w}{\partial x^3} + \frac{\partial v}{\partial x} \frac{\partial^2 w}{\partial x^2} + 2 \nu \frac{\partial^3 w}{\partial x \partial y^2} dy \right) \quad (17)$$

Now, assuming that  $w$  is interpolated by the following forms

$$w(x, y, t_s) = \sum_{j=1}^m w_j^e(t_s) \psi_j(x, y) \tag{18}$$

And substituting  $v = \psi_i(x, y)$  and Eq. (18) into Eq. (17) can obtain the following:

$$\int_{x_a}^{x_b} \int_{y_a}^{y_b} \left[ D \left( \frac{\partial^2 \psi_i}{\partial x^2} \frac{\partial^2 \psi_j}{\partial x^2} + 2 \frac{\partial^2 \psi_i}{\partial x \partial y} \frac{\partial^2 \psi_j}{\partial x \partial y} + \frac{\partial^2 \psi_i}{\partial y^2} \frac{\partial^2 \psi_j}{\partial y^2} \right) w_j^e + \rho h_p \psi_i \psi_j \dot{w}_j^e - \psi_i f + \psi_i q V \left( \Delta \delta'_u \Delta H_v + \Delta H_u \Delta \delta'_v \right) \right] dx dy = 0 \tag{19}$$

The motion equation can be re-arranged in a matrix form as follows:

$$\mathbf{M}\{\ddot{u}\} + \mathbf{K}\{u\} = \mathbf{F}(t) + \mathbf{B}V(t) \tag{20}$$

where the  $u_j$  denotes the nodal values of  $w$  and its derivatives, and the stiffness matrix  $\mathbf{K}$ , mass matrix  $\mathbf{M}$ , and milling force matrix  $\mathbf{F}$  of the element can be obtained as follows:

$$K_{ij} = D \int_{x_a}^{x_b} \int_{y_a}^{y_b} \left( \frac{\partial^2 \psi_i}{\partial x^2} \frac{\partial^2 \psi_j}{\partial x^2} + 2 \frac{\partial^2 \psi_i}{\partial x \partial y} \frac{\partial^2 \psi_j}{\partial x \partial y} + \frac{\partial^2 \psi_i}{\partial y^2} \frac{\partial^2 \psi_j}{\partial y^2} \right) dx dy \tag{21}$$

$$M_{ij} = \int_{x_a}^{x_b} \int_{y_a}^{y_b} \rho h_p \psi_i \psi_j dx dy \tag{22}$$

$$F_i(t) = \int_{x_a}^{x_b} \int_{y_a}^{y_b} \psi_i f dx dy \tag{23}$$

and  $\mathbf{B}$  is the location and characteristic matrix, which is obtained as follows:

$$B_i = \int_{x_a}^{x_b} \int_{y_a}^{y_b} \psi_i q \left( \Delta \delta'_u \Delta H_v + \Delta H_u \Delta \delta'_v \right) dx dy \tag{24}$$

### 3 Design of the control system

#### 3.1 Acceleration feedback-based control system

A closed loop control system containing acceleration sensors and piezoelectric actuators is utilized to control the vibration of the thin plate milling process. The feedback control scheme is illustrated in Fig. 3. The thin plate with piezo actuator attached will vibrate under the excitation by the milling force ( $f$ ), and the vibration is monitoring by the accelerometer. Charge amplifier (YE3822a) is used to amplify the acceleration sensor’s signal to the voltage range of  $-10$  to  $+10$  V, and then the signal is converted into digital data by an A/D (analog to digital) card (Queentest PCIeV1.0). The control function is implemented by a FPGA signal processing card (Queentest PCIeV1.0) and an industrial computer. The output control signal is sent to a D/A (digital to analog) card (Queentest PCIeV1.0) that is used to converts the signals into analog

signal. As the piezoelectric actuator requires high voltage applied to work, a high voltage amplifier (HVA1500/50-1), which could amplify a low voltage signal in the range  $-2.5$  to  $+7.5$  V to a high voltage signal in the range  $-500$  to  $1500$  V, is used between the D/A card and the piezoelectric actuator to drive the actuator.

The A/D card, signal processing card, and D/A card are integrated into one device (Queentest PCIeV1.0). The interface software of the signal processing card is built using ControlDesk and MATLAB/Simulink. The sampling frequency of the whole control system is selected as 10 kHz considering the different performances of each device. In addition, a low-pass filter is used in the signal processing card to eliminate the influence of noises on the output acceleration signal. The control system apparatus is shown in Fig. 4.

The input signal of the control system is generated by acceleration sensor attached at a selected monitoring point on the surface of the thin plate, and the location of the piezoelectric actuator is not at the monitoring point, that is, the actuator cannot directly act on the monitoring point, leading to a time delay of the control system. Moreover, the response and action capability of the apparatus also cause time delay. This time delay will degrade the performance of the control system and will induce instability. In order to overcome the effect of time delay and guarantee the stability of the control system, proportional-derivative (PD) control method is used to compensate for the time delay of the acceleration feedback control.

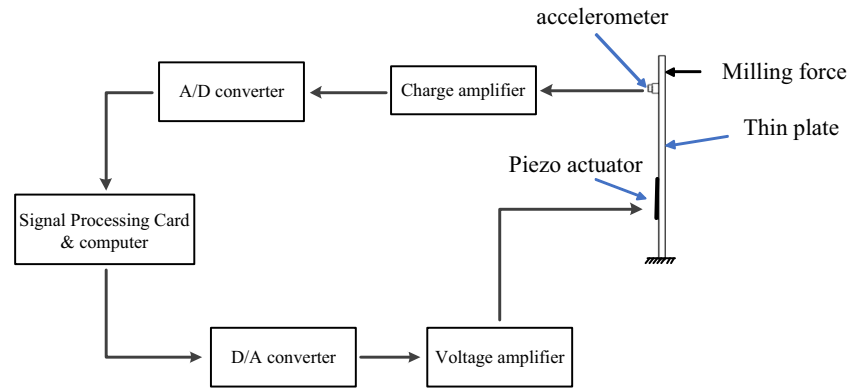
#### 3.2 Time-space varying PD control method

PD control method contains two parts, i.e., proportional control and derivative control. Proportional control is one of the simplest control methods. The output of the controller is proportional to the input signal. But when proportional control is the only control algorithm applied, the system output will have steady-state error. In derivative control, the output of the controller is proportional to the derivative of the input signal (i.e., the rate of variation of the input signal), that is, adding the “derivative term” into control can predict the trend of error change. Thus, the controller with proportional plus derivative can make the control performance of restraining error equal to 0 or even negative in advance, thus avoiding the serious overshoot of the controlled quantity. Therefore, for the controlled object with large inertia or time delay, the proportional plus derivative (PD) controller can improve the dynamic characteristics of the system and achieve a better control performance.

The relationship between output  $u(t)$  and input  $e(t)$  of the controller (signal processing card) utilizing PD control method can be expressed as follows:

$$u(t) = k_p e(t_k) + k_d [e(t_{k+1}) - e(t_k)] \tag{25}$$

Fig. 3 Feedback control scheme



where  $k_p$  is the proportional gain, and  $k_d$  is the derivative gain. The sampling time is 1 ms, which means  $t_{k+1} - t_k = 1$  ms.

In order to control vibration and reduce noise in milling process, the control system should be used to control the response of the cutting point during milling process.

As we know, dynamic characteristics change according to the cutting process (cutting position or cutter-workpiece engagement position) for thin plate milling. Therefore, in order to control the response of the machining point effectively, the parameter of controller should change with the variation of cutter position during milling process and, as a result, the surface finish of workpiece is improved.

Due to the variation of the cutter-workpiece engagement position, the location of acceleration monitor cannot be changed during the milling process and a traditional PD control method with invariant parameter (CPD) could not obtain the optimum vibration suppression performance all the time during the milling process, so a time-space varying PD (VPD) control is utilized, which means the variation of  $k_p$  and  $k_d$  according to the position of milling point is necessary.

To realize the varying PD control, the milling process is discretized into several points by time of the cutting process and area of the thin plate surface. Parameters of the control

system are determined with different values when the cutter moves to different locations.

When the milling cutter moves to different milling points on the cutting path, the value of  $k_p$  should be changed. In order to obtain different values of  $k_p$  during the milling process, a simulation model of the plate-actuator milling system is established according to the Eq. (20).

In the simulation for tuning  $k_p$ , the geometric and material parameters of the workpiece and piezoelectric actuator patch are determined according to experimental conditions, and to simulate the milling force when the milling tool moves to different positions on the milling path, a sinusoidal force (20 Hz) which applied on the milling points is used.

As shown in Fig. 5, 31 milling points are selected on the milling path evenly and tune the corresponding  $k_p$  when the simulation sinusoidal force applied on each selected milling points on the simulation model. Tune values of  $k_p$  for each points to make the vibration response of the corresponding milling points are suppressed to one smaller value, which means, by tuning  $k_p$ , the vibration response of milling points is suppressed to the same level, no matter which selected milling points the simulate force is applied on. From this, the values of  $k_p$  corresponding to each selected milling point  $k_{p1}, k_{p2} \dots k_{p31}$  are obtained.

However, only 31  $k_p$  values are not enough for control system taking a fine vibration control during the whole milling process. An  $k_p$  equation according to the motion of cutter should be derived. From the simulation, it can be found that the change of  $k_p$  is relatively gentle, so in this paper, the equation of  $k_p$  is fitted by polynomial fitting according to 31  $k_p$  values obtained. Experiment shows that quintic polynomial can sufficiently show the changes of  $k_p$  and no higher order is required. The equation of change of  $k_p$  can be written as

$$k_{px} = a_{fit}x^5 + b_{fit}x^4 + c_{fit}x^3 + d_{fit}x^2 + e_{fit}x + f_{fit} \quad (26)$$

where  $x$  represents the distance between the current cutting point and starting point on the cutting path.

Moreover, the values of  $k_d$  are tuned and determined according to experimental apparatus during experiments.

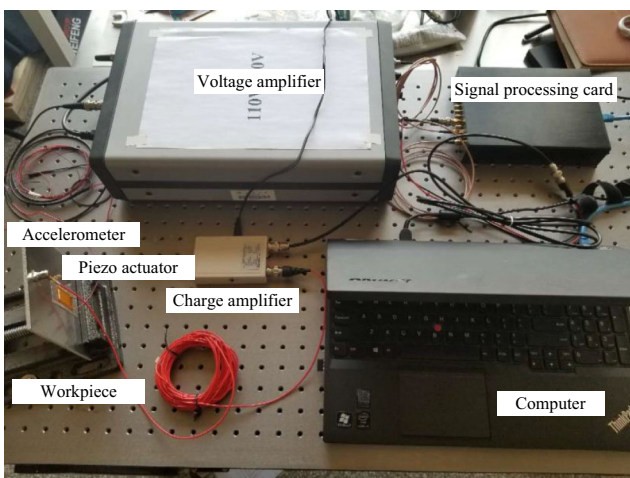
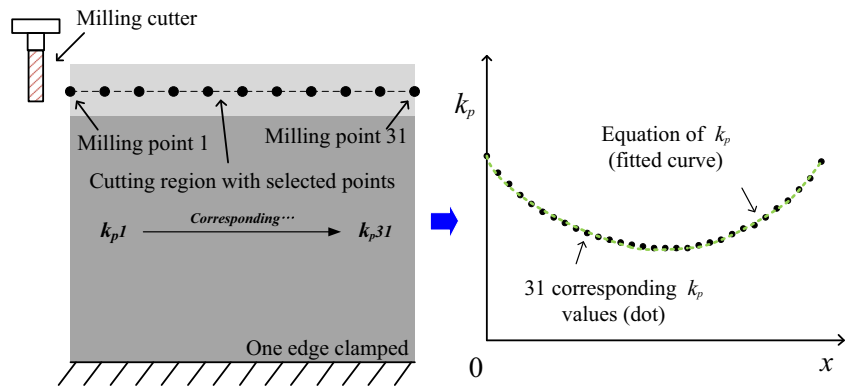


Fig. 4 Control system apparatus

**Fig. 5** Parameters of PD control varying during the milling process



To implement the VPD control method, a control scheme is implemented in Simulink and depicted in Fig. 6. To realize the function that the proportional factor  $k_p$  and the derivative factor  $k_d$  varying according to the cutter position, two global variables which used to assign to  $k_p$  and  $k_d$  are set in the control program.

To summarize the implementation and validation process of the proposed control method, the procedure of how to realize the VPD and verify the effectiveness of it is illustrated in Fig. 7.

## 4 Results and discussions

### 4.1 Description of the simulation and experimental assessment for the validation

#### 4.1.1 Determination of the parameters of the plate-actuator system

To verify the performance of the control system in thin plate milling process, some numerical simulation and experiments are carried out. In order to maximize the control effect of the piezoelectric patch, so that make the control effect of piezoelectric actuator absolutely sufficient for the vibration control, the piezoelectric patch is attached at the position close to the

fixed side in the middle of the workpiece. Moreover, considering the actual attachment method (using special glue) and the electric wire connection, the lower side of the piezoelectric patch is a little distance away from the workpiece’s fixed side. The same geometric and material parameters of the plate-actuator system are determined both in the simulation and experiments.

The geometric properties of plate-actuator system selected in this section are shown in Table 1. The material of thin plate workpiece is Al-Mg alloy 5052 having density  $\rho = 2680 \text{ kg/m}^3$ , Young’s modulus  $E = 700 \text{ GPa}$ , and Poisson ratio  $\nu = 0.330$ , respectively.

Moreover, in order to illustrate the simulation and experimental result clearly, 11 evenly distributed points are selected along the cutter path, as shown in Fig. 8.

#### 4.1.2 Validation of the proposals on the effectiveness of chatter suppression by stability prediction

As seen in Fig. 9, an impact experiment is set up with a one side clamped thin-walled workpiece (Al-Mg alloy 5052,  $120 \text{ mm} \times 120 \text{ mm} \times 4 \text{ mm}$ ), an impact hammer (PCB MIH03 with sensitivity of  $10 \text{ mV/lbf}$ ), and an accelerometer (DYTRAN 3032A with sensitivity  $10.00 \text{ mV/g}$ ). The force and acceleration signals are recorded with a data acquisition system supported by the B&K corporation. Meanwhile, the

**Fig. 6** Control system implemented in Simulink

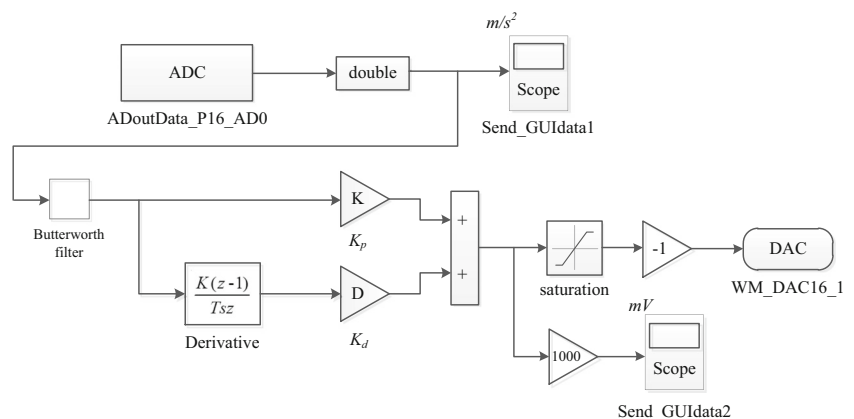
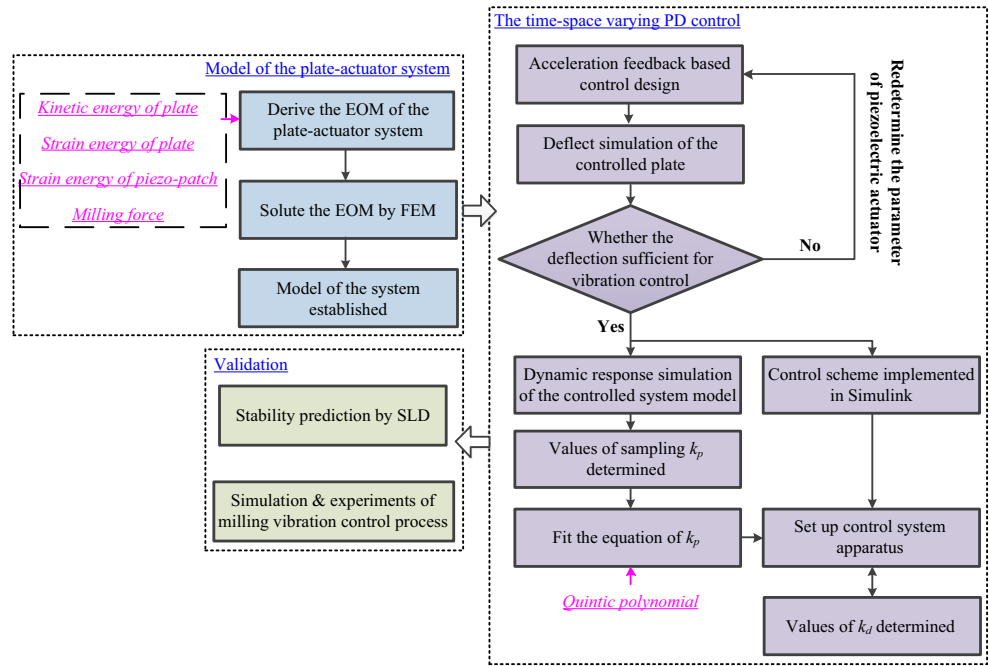


**Fig. 7** Procedure of realizing and verifying the VPD



accelerometer signal is also acquired by the signal processing card (Queentest PCIeV1.0) to implement the proposed control system. Moreover, the piezoelectric actuator is attached on the workpiece, and the location of piezoelectric patch on the workpiece is same as that shown in Table 1.

Both the modal parameters and the loss factor of the system can be obtained from the hammer impact experiment.

Assuming that the system resonates at  $j$ -order modal, if the modal density is not high in this resonant region, other modals' effects can be neglected and the FRF of exciting on point  $n$  and response on point  $r$  of the workpiece can be simplified as

$$H_m(\omega) = \frac{A_{r mj}}{\alpha\omega_j - \omega} + \frac{-A_{r mj}}{-\alpha\omega_j - \omega} \tag{27}$$

where  $A$  is the residue, and

$$\alpha = \sqrt{1 + jg_j} \tag{28}$$

In which  $g_j$  is the loss factor, for the system with small loss factor, there is a relationship between loss factor  $g_j$  and damping ratio  $\zeta$ , which can be written as follows.

$$g_j = 2\zeta \tag{29}$$

The damping ratio of the plate-actuator system can be extracted with the half-power bandwidth method.

To make the calculation simple, the modal shape of the system at milling position point is assumed to be one. Moreover, the exciting point and the response point are considered as the same position points. Then, the modal

**Table 1** Geometric properties of plate-actuator system selected

	length $L$ (mm)		width $W$ (mm)		thickness $t_p$ (mm)
Thin plate	120		120		4
Piezoelectric actuator	position(mm)				thickness $t_a$ (mm)
	$u_1$	$u_2$	$v_1$	$v_2$	0.4
	50	70	20	58	
Acceleration sensor	position(mm)				
	$x_{acc}=60$		$y_{acc}=100$		



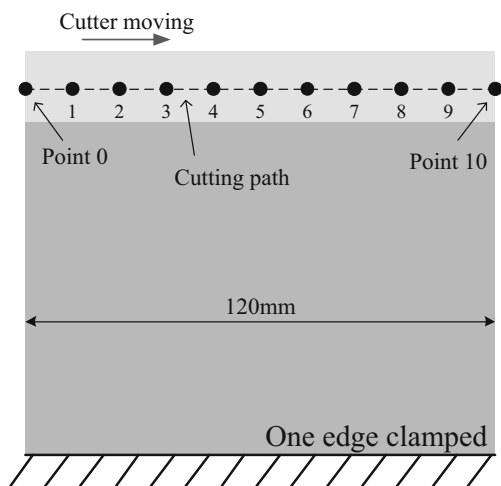


Fig. 8 Position point distribution

mass  $m_{nj}$  at the point can be obtained as

$$m_{nj} = \frac{1}{|2A_{nj}\alpha|} \tag{30}$$

Correspondingly, the modal stiffness  $k_{nj}$  and modal damping  $c_{nj}$  at the point are derived as

$$k_{nj} = m_{nj}\omega_j^2 \tag{31}$$

and

$$c_{nj} = 2m_{nj}\zeta\omega_j \tag{32}$$

The impact experiment is implemented with two cases: case I, the control system is off, and case II, the control system working with proposed varying PD methods.

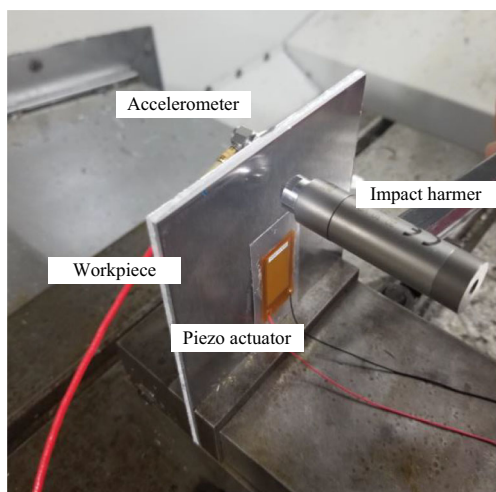


Fig. 9 Impact experiment

### 4.1.3 Validation of the proposals on the effectiveness of milling vibration suppression

To validate the effectiveness of the proposals in milling process, dynamic response simulation of the controlled plate-actuator system and milling experiments is carried out.

In order to compare the effectiveness of different control methods, a response simulation of the plate-actuator system is carried out. There are three control conditions applied in the simulation, which are no controlled, constant PD control (CPD), and proposed PD control (VPD) with  $k_p$  changing according to the  $k_p$  equation obtained by the method mention in Sect. 3.2.

Milling experiment is also carried out to verify the viability and effectiveness of suppressing the milling vibration of the proposals. The milling vibration control experiment is carried out on a vertical CNC machining center (DAEWOO ACE-V500) with the maximum spindle rotation of 30,000 rpm. A cemented carbide cylindrical end mill with four cutting edges, 12 mm diameter, 45° helix angle, the length of tooth 30 mm, and overhang 45 mm is used. To measure the vibration of the plate, a laser sensor (Keyence LKM-G30) with a resolution of 10 nm, minimum sample period of 20 is used to measure the displacement. The milling experimental setup is shown in Fig. 10. The thin plate and piezoelectric actuator in the cutting tests take the same size and parameter as those determined above. Milling mode is side milling with Feed-rate of 600 mm/min. To validate the performance of proposed control system, three conditions are selected, where the control system is off, constant PD control is used, and the proposed vary PD control is used, respectively.

On unprocessed surface of the plate surface, 11 evenly distributed position points referred in Sect. 4.1 are signed from left to right.

The cutting parameters of the stable milling experiments have been set to depth of cut 0.2 mm, spindle speed 7000 rpm, and feed rate 720 mm/min. The cutter will take 10 s to move from point 0 to point 10 in milling process.

## 4.2 Validation of proposed method

### 4.2.1 Determination of the parameters of the plate-actuator system

Figure 11 shows the static deflection of the plate-actuator system at the top side of the thin-walled plate in the condition of 500 V, 900 V, and 1200 V applied on the actuator, respectively. From Fig. 11, it can be found that the deformation of the plate caused by the piezoelectric actuator is sufficient for suppressing the cutting vibration in milling process. Furthermore, the deformation increase with the increase of voltage applied on the piezoelectric actuator and different deformation of the plate at different points. Therefore, in order to control the

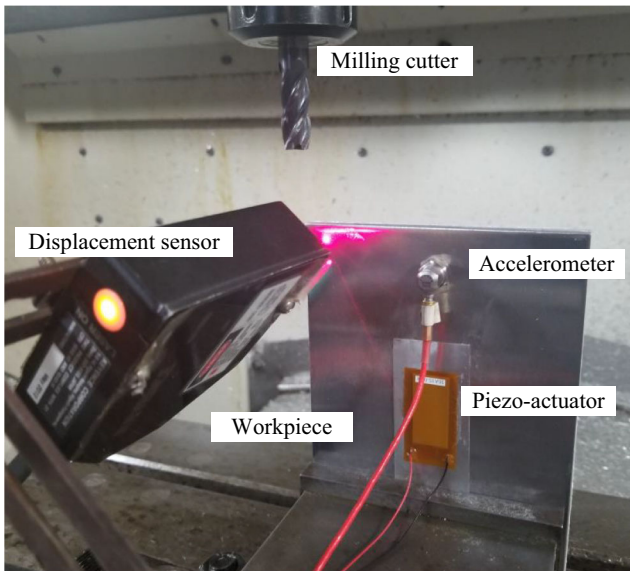
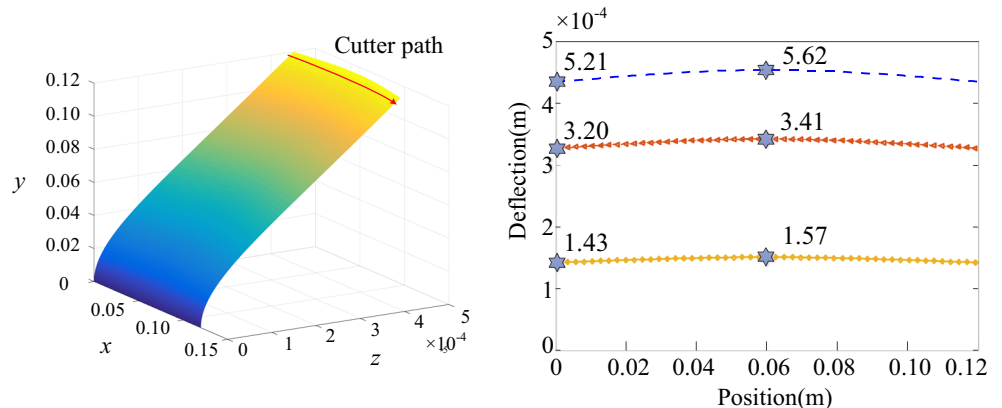


Fig. 10 Milling experiment

response of the machining point effectively, the parameter of the PD control should change with the variation of cutter position during milling process, which means the time-space varying PD control.

The simulation of tuning the  $k_p$  mentioned in Sect. 3.2 is carried out; in the simulation, the model of the milling vibration control system has geometric properties all same as those mentioned in Table 1, and the cutter path (cutting area during milling process) is simplified as a straight line on processing surface which is parallel to and 3 mm from the top edge of the thin-walled workpiece. By the simulation, 31 corresponding values of  $k_p$  are obtained, and then the equation of change of  $k_p$  (Eq. 20) in the milling process is fitted using the 31 values of  $k_p$ . Here, values of each parameter for the  $k_p$  equation are as follows:  $a_{fit} = -5.122e-9$ ,  $b_{fit} = -6.604e+4$ ,  $c_{fit} = 1.585e+4$ ,  $d_{fit} = -818.4$ ,  $e_{fit} = -15.91$ , and  $f_{fit} = 3.938$ .

Fig. 11 Static deflection at the top side of the thin-walled plate. Yellow line: voltage = 500 V; red line: voltage = 900 V; blue line: voltage = 1200V



As mentioned above, 11 distributed points along the cutter path are selected, and according to the fitted  $k_p$  equation,  $k_p$  of different milling points are obtained; it can be noted that the cutting points that farther from the piezoelectric actuator have a higher  $k_p$ . Moreover, considering the characteristic of plate and apparatus of control system,  $k_d$  of different milling points are estimated. The  $k_p$  and  $k_d$  of different milling points are shown in Table 2. It should be noted that, in the numerical simulation, the milling process is not perfect continuous but divided into as many steps as possible, and in this analysis, as many values as possible of  $k_p$  and  $k_d$  related to milling process are also determined.

#### 4.2.2 Validation of the proposals on the effectiveness of chatter suppression by stability prediction

As mentioned above, impact experiments were carried out to get the modal parameters of the workpiece-actuator system. The position point 1 and point 5 referred in Sect. 4.1 is selected as the experimental and extracting points. Figure 12 shows the FRFs of the workpiece obtained from the impact experiments.

Based on the impact experiment, the modal parameters of the workpiece-actuator system at the second order under two control cases are extracted and shown in Table 3.

From Table 3, it can be easily found that modal parameters at middle of the cutter path is larger than that at the starting or ending position of the cutter path, and the proposed control method has a significant impact on raising the modal parameters at both points.

According to the modal parameters extracted and shown in Table 3, the stability lobe diagram of the cutting point 1 and point 5 is obtained and illustrated in Fig. 13. The figure shows that the proposed VPD method managed to increase the stability area of milling process at both the starting/ending and the middle of the milling process.

**Table 2** Parameters of PD at different points

Position point	0	1	2	3	4	5	6	7	8	9	10
$k_p$	3.94	3.66	3.28	2.93	2.69	2.60	2.69	2.93	3.28	3.66	3.94
$k_d$	0.7	0.7	0.6	0.5	0.5	0.5	0.5	0.5	0.6	0.7	0.7

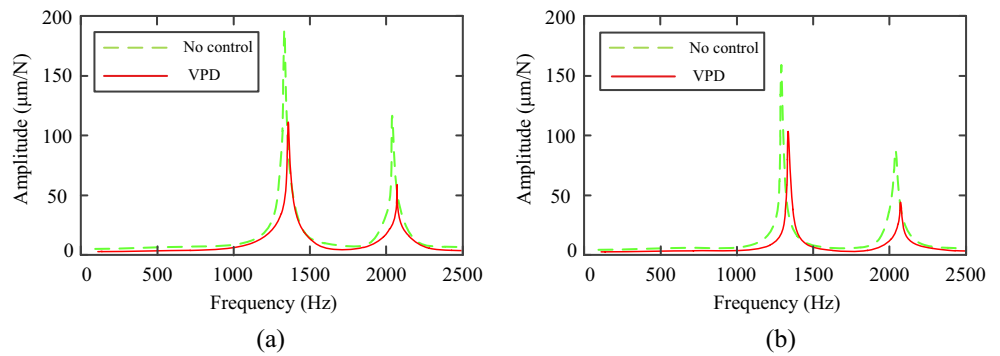
**4.2.3 Validation of the proposals on the effectiveness of milling vibration suppression**

Figure 14 shows the simulation results of the vibration of milling point (processing point) in the condition of no controlled, constant PD control (CPD), and proposed PD control (VPD), respectively. It can be seen that, with CPD on, the vibration of milling point has been suppressed, but not evenly suppressed, and when the cutting position moves to the point close to the actuator, the suppression effect is better, but when the cutter moves to the area far from the actuator, the suppression effect is poor. This is

cutting area is also smaller than expected. On the other hand, when the VPD control is utilized, the dynamic vibration response of the cutting system is effectively and evenly suppressed. This is because that the VPD control method considers the changing of milling cutting position during the whole milling process.

Figures 15, 16, and 17 show displacement signals when the laser sensor measuring at the position points 1, 5, and 9 during milling process with different control conditions, respectively. It is easy to find from Figs. 15, 16, and 17 that large vibration occurred during milling process with selected cutting parameter without any vibra-

**Fig. 12** FRFs of the workpiece-actuator system. **a** FRFs of point 1. **b** FRFs of point 2



because both accelerometer and piezoelectric actuator are attached at the fixed position, which are unchangeable during the whole milling process. When the milling cutter moves to the area far from the accelerometer and actuator, the vibration measured by accelerometer is smaller than the that occurring on the cutting area, and the workpiece deflection applied by the actuator at starting and ending

tion control method; when cutter moves to the position near point 3 and point 9, serious vibration occurred; and when the cutter move into the area from point 9 to point 10, even chatter is found in Figs. 15 and 17. Moreover, when the cutter moves to some specific area, such as the area near point 4 and point 8, shown in Fig. 16, serious vibration even chatter could occur. The selected

**Table 3** Modal parameters of the workpiece-actuator system at the second order

Position point number	Without control			Proposed varying PD control		
	Modal mass (kg)	Modal stiffness ( $\times 10^6$ N/m)	Modal damping (N s/m)	Modal mass (kg)	Modal stiffness ( $\times 10^6$ N/m)	Modal damping (N s/m)
1	0.0035	0.6486	2.9363	0.0072	1.5696	7.0163
5	0.0114	2.1126	9.5640	0.0167	3.6407	16.2744

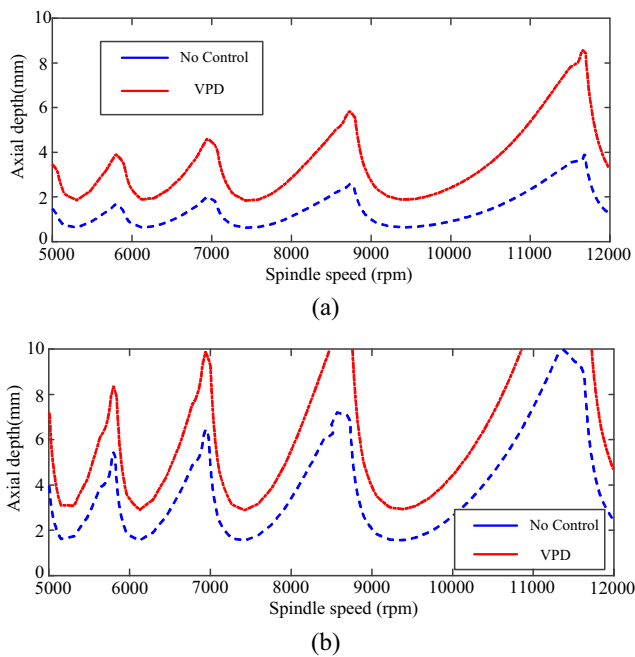


**Fig. 13** SLD with different control conditions. **a** SLD of point 1. **b** SLD of point 5

workpiece has a very poor stiffness; from the experiment result, it can be seen that surface integrity of processed workpieces is particular poor.

When the CPD method is used into the milling process, as shown in Figs. 15, 16, and 17, the cutting vibration is suppressed greatly, especially when the cutter moving from point 3 to point 9; however, the CPD method shows a poor performance when the cutter is cutting at the starting or ending position of the cutter path. Large vibration still occurred when the cutter moves from point 0 to point 1 and point 9 to point 10.

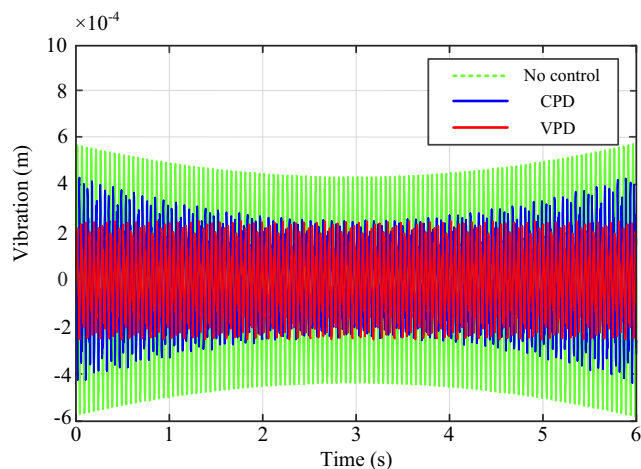


**Fig. 14** Vibration of processing point in different control conditions

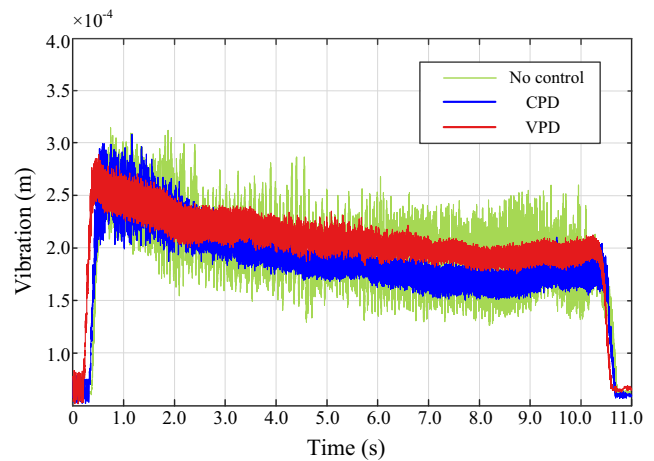


**Fig. 15** Displacement response at position point 1 during milling process

Compared with no control and CPD control conditions, the VPD control perform excellent in suppressing the milling vibration significantly and evenly during the whole milling process. As shown in Figs. 15, 16, and 17, no matter which position the cutter is cutting at, the control system restrains the milling vibration successfully, and all three displacement response signal measuring at point 1, point 5, and point 9 shows little vibration amplitude.

Moreover, to illustrate the comparison of three control conditions more clearly, histograms showing the amplitude of the vibration measured by displacement sensor at point 1 and point 5, respectively, are depicted in Fig. 18.

From the histograms, it can be found that no matter where the displacement sensor measures on, the results are relatively same and both the method CPD and VPD can suppress vibration in the milling process. Comparing the vibration suppression effect of the two methods, the

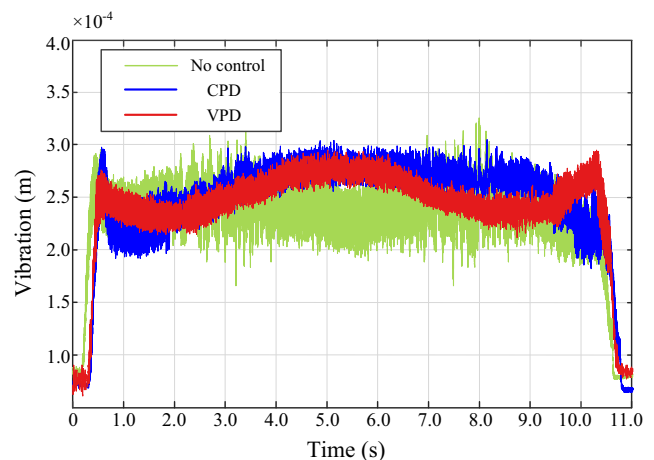


**Fig. 16** Displacement response at position point 5 during milling process

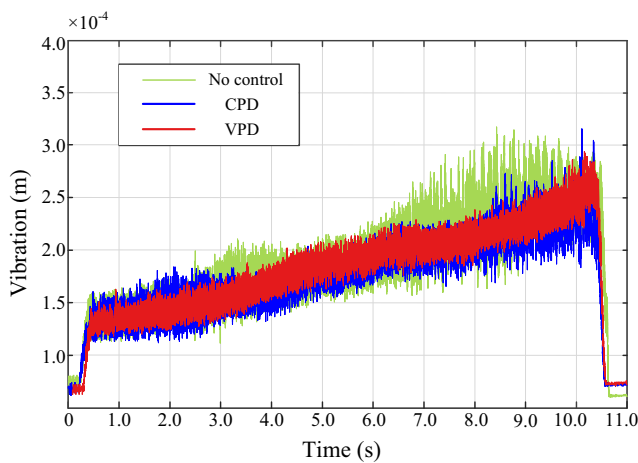


Fig. 17 Displacement response at position point 9 during milling process

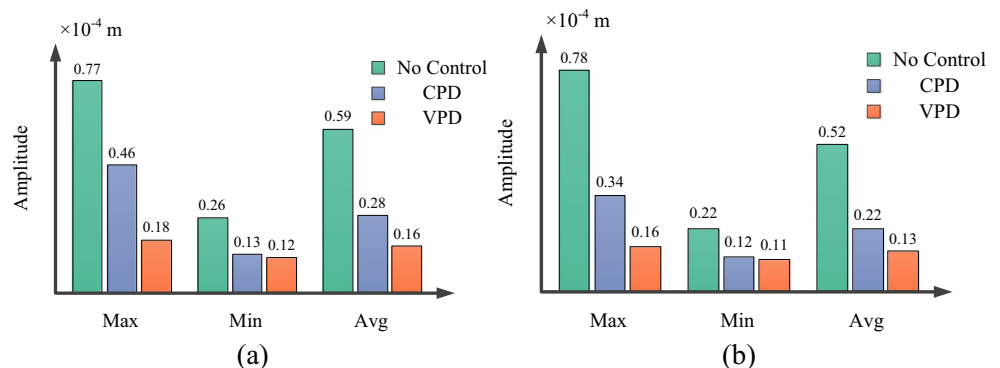
minimum suppressed amplitude of the two methods are approximately the same, that is, the optimal suppression effect of the two methods are not much different in the whole cutting process. Generally, the optimal vibration suppression effect of CPD and VPD occurs when the tool moves to the middle of cutting path on the workpiece. This is because, firstly, the cutting is more stable when the tool moves to the middle part of the workpiece, and secondly, the middle part is the nearest to the piezoelectric actuator; when the cutting moves to here along the cutting path, the vibration suppression effect exerted by CPD is the most obvious. However, the average and maximum suppressed amplitudes obtained by CPD are obviously larger than those obtained by VPD, especially the maximum amplitude. In the processing area far from the attached piezoelectric patch, the suppression effect of CPD is very poor, and the maximum suppressed amplitudes obtained by CPD usually occur in this area. It can be seen from the diagrams that the maximum and minimum suppressed amplitudes obtained by CPD are quite different, which will lead to the machined workpiece having an uneven surface quality. Moreover, the large

amplitude vibration will cause poor surface integrity and even induce severe chatter. Comparing the average suppressed amplitude obtained by CPD and VPD, it can be found that the average suppressed amplitude of CPD is obviously larger than that of VPD while the minimum suppressed amplitudes of the two control methods are almost the same, which means effect of vibration suppression of VPD is much better than that of CPD.

### 5 Conclusions

In thin-walled workpiece milling process, the cutting position is time varying. Normal closed-loop control system, which applies constant control parameter, cannot effectively suppress machining vibration and improve surface finish in this condition. This is caused by two key factors. One is the dynamic characteristics of the cutting system changing according to the cutting process. The other is cutter-workpiece engagement position is changing while the location of sensor and piezoelectric actuator are fixed. Therefore, in order to control the response of the machining point effectively, the parameter of controller should change with the variation of cutter position during milling process. In this paper, an active milling vibration control system based on the acceleration feedback control and using piezoelectric patch as actuator is designed to suppress vibration of the thin-wall workpiece milling. A time-space varying PD (VPD) control method is presented and utilized as the control algorithm of the controller. This proposed VPD control method can solve the problem of the time variant of dynamic characteristics and the position limit of sensor and actuator during milling process. Compared with the traditional constant PD control method (CPD), the proposed VPD method performs better in the vibration suppression for thin-walled workpiece milling process and contributes to surface finish of workpiece. By using simulation and experimental verification, the accuracy and efficiency of the control system are validated.

Fig. 18 Amplitude of suppressed vibration under 3 control conditions. a Measured at point 1. b Measured at point 5



**Funding information** The authors are grateful to the financial supports of the National Natural Science Foundation of China (no. 51575319), the Major projects of National Science and Technology (Grant No. 2019ZX04001031), Natural Science Outstanding Youth Fund of Shandong Province (Grant No. ZR2019JQ19), and the Key Research and Development Plan of Shandong Province (no. 2018GGX103007). The authors declare that there is no conflict of interest.

### Compliance with ethical standards

**Conflict of interest** The authors declare that they have no conflict of interest.

### References

- Altintas Y, Budak E (1995) Analytical prediction of stability lobes in milling. *Ann CIRP* 44:357–362
- Budak E, Altintas Y (1998) Analytical prediction of chatter stability in milling – part I: general formulation. *J Dyn Syst Meas Control* 120(1):22–30
- Zhou X, Zhang DH, Luo M, Wu BH (2018) Chatter stability prediction in four-axis milling of aero-engine casings with bull-nose end mill. *Chin J Aeronaut* 28(6):1766–1773
- Long X, Jiang H, Meng G (2013) Active vibration control for peripheral milling processes. *J Mater Process Technol* 213(5):660–670
- Liu KJ, Rouch KE (1991) Optimal passive vibration control of cutting process stability in milling. *J Mater Process Technol* 28:285–294
- Sathianarayanan D, Karunamoorthy L, Srinivasan J, Kandasami K, Palanikumar K (2008) Chatter suppression in boring operation using magnetorheological fluid damper. *Mater Manuf Process* 23(4):329–335
- Mei DQ, Kong TR, Shih AJ, Chen ZC (2019) Magnetorheological fluid controlled boring bar for chatter suppression. *J Mater Process Technol* 209(4):1861–1870
- Mei DQ, Yao ZH, Kong TR, Chen ZC (2010) Parameter optimization of time-varying stiffness method for chatter suppression based on magnetorheological fluid-controlled boring bar. *Int J Adv Manuf Technol* 46(9–12):1071–1083
- Min W, Ting-Qi G, Jia F, Wei-Hong Z (2019) On improving chatter stability of thin-wall milling by prestressing. *J Mater Process Technol* 264:32–44
- Shamoto E, Mori T, Nishimura K, Hiramatsu T, Kurata Y (2010) Suppression of regenerative chatter vibration in simultaneous double-sided milling of flexible plates by speed difference. *CIRP Ann Manuf Technol* 59(1):387–390
- Kiran K, Dragos A, Adib B (2013) A solution for minimising vibrations in milling of thin walled casings by applying dampers to workpiece surface. *CIRP Ann Manuf Technol* 62(1):415–418
- Wan M, Dang XB, Zhang WH (2018) Optimization and improvement of stable processing condition by attaching additional masses for milling of thin-walled workpiece. *Mech Syst Signal Process* 103:196–215
- Yuan H, Wan M, Yang Y (2019) Design of a tunable mass damper for mitigating vibrations in milling of cylindrical parts. *Chin J Aeronaut* 32:748–758
- Wang C, Zhang X, Liu Y, Cao H, Chen X (2018) Stiffness variation method for milling chatter suppression via piezoelectric stack actuators. *Int J Mach Tools Manuf* 124:53–66
- Sajedi Pour D, Behbahani S (2016) Semi-active fuzzy control of machine tool chatter vibration using smart MR dampers. *Int J Adv Manuf Technol* 83(1-4):421–428
- Tewani SG, Rouch KE, Walcott BL (1995) A study of cutting process stability of a boring bar with active dynamic absorber. *Int J Mach Tool Manu* 35(1):91–108
- Zhang YM, Sims ND (2005) Milling workpiece chatter avoidance using piezoelectric active damping: a feasibility study. *Smart Mater Struct* 14:65–70
- Venter GS, Silva LMDP, Carneiro MB, Maira MDS (2017) Passive and active strategies using embedded piezoelectric layers to improve the stability limit in turning/boring operations. *Int J Adv Manuf Technol* 89(9-12):2789–2801
- El-Sinawi AH, Kashani R (2005) Improving surface roughness in turning using optimal control of tool's radial position. *J Mater Process Technol* 167:54–61
- Brecher C, Manoharan D, Ladra U, Kopken H-G (2010) Chatter suppression with an active workpiece holder. *Prod Eng* 4:239–245
- da Silva MM, Cervelin JE, Calero DP, Coelho RT (2013) Availability study on regenerative chatter avoidance in turning operations through passive and active damping. *Int J Mechatron Manuf Syst* 6(5/6):455–473
- Tanaka H, Obata F, Matsubara T, Mizumoto H (1994) Active chatter suppression of slender boring bar using piezoelectric actuators. *JSME Int J Ser C* 37(3):601–606
- Crawley EF, de Luis J (1987) Use of piezoelectric actuators as elements of intelligent structures. *AIAA J* 25(10):1373–1385
- Rofoei FR, Nikkhoo A (2009) Application of active piezoelectric patches in controlling the dynamic response of a thin rectangular plate under a moving mass. *Int J Solids Struct* 46(11-12):2429–2443
- Qiu ZC, Han JD, Zhang XM, Wang YC, Wu ZW (2009) Active vibration control of a flexible beam using a non-collocated acceleration sensor and piezoelectric patch actuator. *J Sound Vib* 326(3-5):438–455
- Song QH, Ai X, Tang WX (2011) Prediction of simultaneous dynamic stability limit of time-variable parameters system in thin-walled workpiece high-speed milling processes. *Int J Adv Manuf Technol* 55:883–889
- Song Q, Shi J, Liu Z, Yi W (2016) A time-space discretization method in milling stability prediction of thin-walled component. *Int J Adv Manuf Technol* 89:1–15

**Publisher's note** Springer Nature remains neutral with regard to jurisdictional claims in published maps and institutional affiliations.